USBPO U.S. BURNING PLASMA ORGANIZATION

eNews

December 12, 2011 (Issue 61)

CONTENTS

Dear Burning Plasma Aficionados:
This newsletter provides a short update on U.S. Burning Plasma Organization activities. E-News is also available online. Comments on articles in the newsletter may be sent to the Editor (Dylan Brennan) Assistant Editor (Rita Wilkinson). Thank you for your interest in Burning Plasma research in the U.S.!

Director's Corner by C. M. Greenfield

Looking back and looking forward

2011 was a busy year in burning plasma science. ITER continued to move forward into its construction phase, while the worldwide fusion community continued to address scientific and technical issues toward our common goal of being ready to carry out a successful research program on ITER.

 

Before and after: The ITER site in 2008 (left) and in November 2011 (right). Photos © ITER Organization.

As ITER continued to progress, so too has US burning plasma science. As we saw at the recent APS meeting, high quality and relevant research supporting ITER is being carried out throughout our community.

There have been changes in the US Burning Plasma Organization, too. As you remember, our esteemed previous Director, Jim Van Dam, left the University of Texas and the USBPO in September to join the US Department Of Energy as the new Director of Research for Fusion Energy Sciences. I was appointed Director, and Amanda Hubbard replaced me as Deputy Director. Looking forward to next year, we are considering some initiatives to make the USBPO more effective, including formation of some new task groups. You will hear more in 2012. Of course, we are always interested in your suggestions for how better to use the USBPO as a tool to accomplish our mission to *advance the scientific understanding of burning plasmas and ensure the greatest benefit from a burning plasma experiment by coordinating relevant U.S. fusion research with broad community participation*.

APS-DPP Conference

The 53rd Annual Meeting of the APS Division of Plasma Physics was held last month in Salt Lake City, with two sessions being organized by the USBPO.

Many of you attended the USBPO Town Meeting on ITER Status on Tuesday evening. Presentations included:

- Joseph Snipes, *Senior Scientific Officer, Plasma Operations, of the ITER Organization*, "Latest Developments on ITER"
- David Rassmussen, *Heating Fueling, and Disruption Mitigation Manager for the US ITER Project*, "Overview of ITER Heating and Current Drive Systems"
- Réjean Boivin, *Chair, ITPA Topical Group on Diagnostics*, "ITER Diagnostics: Current Perspective"
- Charles Greenfield, *Director, US Burning Plasma Organization*, "US Contributions to ITER R&D and Open Scientific Opportunities"

The talks were followed by an open discussion period.

The following morning, our fourth annual Research in Support of ITER contributed oral session was held, including talks on a broad range of topics encompassing the major facilities, separate research directly supported by ITER, and talks from our colleagues at JET and ASDEX-U.

I hope to be able to post all of the slides from these talks on the USBPO website soon.

ITER Council Meeting

The ITER Council met in Cadarache on November 17 and 18. Items under discussion included recent recommendations by the STAC (Science and Technology Advisory Committee) and MAC (Management Advisory Committee), as well as the positive outcome of a public inquiry that is a key step toward full licensing of ITER. The Council commented on developments at ITER, noting "the highly productive period of project execution" under the new, reorganized, and streamlined ITER Organization leadership. This ninth ITER Council meeting was also the end-of-term for the Chairman, Evgeny Velikhov. He will be succeeded in this position by Hideyuki Takatsu, the Deputy Director-General of the Japanese Domestic Agency, with Edmund Synakowski, Associate Director of Science for Fusion Energy Sciences within the US Department of Energy, becoming the new Deputy Chair of the ITER Council. Also the new Chairs of the ITER Council's MAC and STAC will be Dr. Ranjay Sharan and Prof. Joaquin Sanchez, respectively.

…more about ITER

ITER has posted a number of interesting videos on their website, including an animation of the assembly of the ITER cryostat. Also, the 200th issue of ITER Newsline was recently released, with a retrospective of the first 199 issues giving a nice summary of progress to date.

ITER Postdoctoral Fellowships

Applications are now being accepted for the Principality of Monaco/ITER Postdoctoral Research Fellowships. This can be a fantastic opportunity for early career scientists and engineers to jump right to the forefront of burning plasma research. For more information, and to apply, please visit the website announcing the fellowships.

European ITER Funding

It was reported this week that a deal was struck within Europe to fully fund their share of the costs of ITER during 2012-13. The full story is available in the December 2 issue of ITER Newsline.

Holiday Greetings

This is the last issue of eNews for the calendar year 2011. We wish you a happy and safe holiday.

USBPO Topical Group Highlights

(Editor's Note: The BPO Modeling and Simulation Topical Group works to facilitate U.S. efforts to develop and apply numerical codes to understand present fusion-related experiments and to predict the performance of future experiments and devices [leaders are Dylan Brennan and Dave Mikkelsen]. This month's Research Highlight by Tariq Rafiq and Arnold Kritz discusses their most recent simulations of ITER discharges and the predicted fusion power, including advanced transport simulations and details of how the fusion power varies with different heating mechanisms, the resultant equilibrium states, and the timing of their deposition. Ratios of fusion power to input power up to 10 are found for target ITER operational scenarios.)

Simulations of ITER Plasma Discharge Scenarios

T. Rafiq and A. H. Kritz *(Lehigh University)*

The objective of this modeling is to prepare for the commissioning of ITER and to plan for the burn stages of ITER operation. The combination of the PTRANSP and TSC codes has been used in joint PPPL/Lehigh studies to simulate ITER target steady state, hybrid and H-mode discharges from ramp-up through flat-top [1-3]. The target steady state discharges are discharges with limited ohmically driven current, and the hybrid discharges are H-mode discharges with a lower plasma current than the plasma current in the standard 15 MA ELMy H-mode discharges.

The PTRANSP code used in these simulations was developed in a collaborative effort during the past 5 years involving GA, LLNL, Princeton and Lehigh. The objective has been to increase the predictive capability of the analysis TRANSP code in order to provide the community with a tool for carrying whole device integrated predictive modeling on the discharge time scale. Currently the same code base provides users with both the TRANSP interpretive capability and PTRANSP predictive capability.

The free-boundary equilibrium, coil currents, temperature and magnetic q-profile, from start-up through the flat-top stage, was computed using the TSC code. The PTRANSP code is then run either in analysis mode or in predictive mode [1-2]. In predictive mode, the PTRANSP code is used to compute temperature, magnetic q and toroidal rotation profiles using either the new Multi-Mode (MMM7.1) or the GLF23 anomalous transport models. GLF23 is a quasilinear gyrofluid model that is used to compute the anomalous transport driven by ion and electron temperature gradient modes and trapped electron modes [4]. The MMM7.1 is a multi-fluid theory based transport model which, in addition to computing the anomalous transport associated with modes included in the GLF23 model, also includes transport associated with the ideal MHD and drift resistive inertial ballooning modes [5]. External heating and current drive involve injection of energetic neutral beams, ion cyclotron, lower hybrid (LH), and electron cyclotron (EC) waves. In analysis mode PTRANSP is used to compute toroidal angular rotation profiles and refine power deposition and current drive profiles for use in subsequent TSC simulations [3].

Simulations of hybrid discharges, using either the MMM7.1 model or the GLF23 model (with the assumption that the GLF23 momentum transport is $\chi_{\phi} = \chi_{\phi,GLF23}$) indicate that 500MW of fusion power is achieved with 53 MW input power in 1000 sec simulations [1], corresponding to Q~10 where Q=fusion power/input power. In simulations employing the GLF23 model in which the momentum transport is simply set equal to the ion thermal transport, $\chi_{\phi} = \chi_{i,GLF23,}$ a lower value of fusion power, 300 MW, is predicted.

In target steady state discharges, it is found that an improvement in fusion power production and a significant increase in fusion Q occur when RF heating and current drive are turned off after 500 seconds [1]. The peak fusion power production is 178 MW corresponding to a fusion Q of 2.1 when radio frequency heating (RF) is kept on during the entire 1000-second discharge and anomalous transport is predicted using the MMM7.1. When the RF power is turned off at 500 seconds, the fusion power predicted at 1000 seconds is 226 MW corresponding to a fusion Q of 6.8. Similar results are obtained using the GLF23 model. The increase in fusion power, with the radio frequency source turned off at 500 seconds, results because since the total current is fixed at 9 MA, when the lower hybrid (LH) current drive, which occurs in the outer third of the plasma, is not available, there is a redistribution of the current resulting in a more centralized current profile. As a result there is a flattening of the q profile and a reduction in magnetic shear resulting in a stabilizing effect on the anomalous transport. Simulations of steady state discharges also indicate an increase in fusion power when LH input power is replaced with EC power [2]. This increase is also understood in terms of the differences in current profiles associated with the change of heating power.

A study has been carried out to examine the sensitivity of fusion power production to the height of the H-mode pedestal and to the boundary rotation frequency for ITER steady state discharges [2]. As the pedestal temperature increases in steady state discharges, there is an associated increase in bootstrap current in the pedestal region. If the total current is maintained constant, the core current decreases. It is shown that this decrease in core current can negate the improvement in fusion power production associated with an increase in pedestal height that might be expected given the stiff nature of the GLF23 and MMM7.1 transport models. It will be shown below that the dependence of fusion power on pedestal temperature in ITER H-mode discharges is significantly different than the predicted dependence for steady state discharges. Formation of an internal transport barrier in temperature and rotation frequency is predicted using the MMM7.1 model in the target steady state discharges. A similar internal transport barrier is not found when simulations are carried out using the GLF23 transport model.

Simulations have been carried out in order to study the dependence of heat deposition and current drive with varying ion cyclotron resonance frequency (ICRF), number of poloidal modes, beam orientation, number of Monte Carlo particles and electron cyclotron resonance heating (ECRH) azimuthal launch angles [3]. These simulations obtain boundary conditions provided by the TSC code and utilize the PTRANSP code in an analysis mode.

Simulations of 15 MA ELMy H-mode discharges have also been carried out to determine the predicted fusion power in these discharges as well as the dependence of fusion power on the height of the H-mode pedestal temperature. Fusion power production predicted using MMM7.1 and GLF23 models is in the range of 500 MW to 650 MW depending on the pedestal temperature with 53 MW of input heating power. In contrast to the steady state results the fusion power predicted using the GLF23 model does increase with increasing pedestal temperature and the fusion power predicted using the MMM7.1 model is relatively insensitive to pedestal temperature as shown in Figs. 1a and 1b below. The insensitivity of

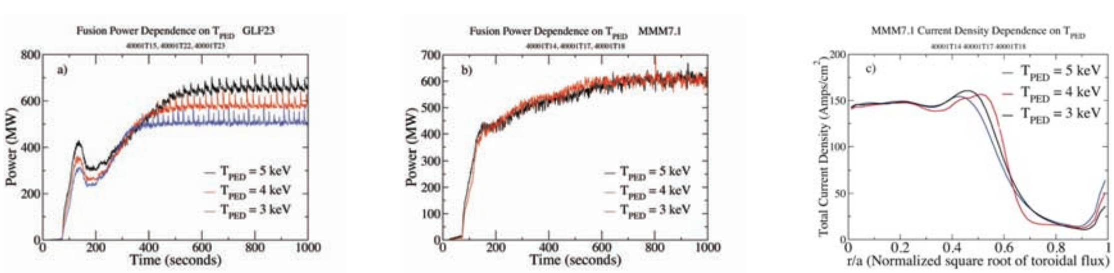

Figure 1: Fusion power production as a function of time using the GLF23 anomalous transport model a), MMM7.1 model b) and Total Current Density as a function radius at 1000 seconds c) with T_{PED} equal to 3, 4 and 5 keV.

fusion power to pedestal temperature in the MMM7.1 simulations results are due to the limited change in core plasma current density, as shown in Fig. 1c, and the limited change in toroidal rotation frequency.

The oscillations that occur in the fusion power are associated with the sawteeth oscillations that occur in the temperature.

ACKNOWLEDGMENT

This USBPO highlight is dedicated to the memory of Doug McCune and Glenn Bateman whose tireless efforts enabled carrying out whole device modeling predictive simulations.

REFERENCES

1. *Integrated Modeling for Prediction of Optimize ITER Performance*, by A.H. Kritz, T. Rafiq, C. Kessel, G. Bateman, D.C. McCune, R.V. Budny, A.Y. Pankin, Nucl. Fusion **51,** 12300, (2011).
2. *Effect of pedestal height and internal transport barriers on ITER target steady state simulations,* Physics of Plasmas, **18,** 112508 (2011) by T. Rafiq, A.H. Kritz, C. Kessel, G. Bateman, D.C. McCune, R.V. Budny.
3. *Study of Heating and Fusion Power Production in ITER Discharges,* AIP Conference Proceeding 1392 IFP-CNR - CHALMERS Workshop on Nonlinear Phenomena on Fusion Plasmas (2011) by T. Rafiq, A.H. Kritz, C. Kessel, G. Bateman, D.C. McCune, R.V. Budny, and A.Y. Pankin.
4. J. Weiland, *et al*. Nucl. Fusion **49**, 965933 (2009), G. Bateman, *et al*. Plasma Phys. Control. Fusion **48**, A93 (2006); W. Horton, *et al*. Phys. Plasmas **7**, 1494 (2000); T. Rafiq, *et al*. Phys. Plasmas **17**, 082511 (2010).
5. R.E. Waltz, *et al*. Phys. Plasmas **4**, 2482 (1997); G. M. Stabler, *et al*. Nucl. Fusion **37**, 287 (1997); J. E. Kinsey, *et al*. Phys. Plasmas **12**, 052503-1 (2005).

ITPA Reports

Summary of the 7th Meeting of the ITPA Transport and Confinement Topical Group

S. Kaye *(Princeton Plasma Physics Laboratory)*

The 7th meeting of the ITPA Transport and Confinement Topical Group was held at the ITER Headquarters, Cadarache, France from October 5 to 7, 2011. The meeting was attended by over 30 physicists from the U.S., Europe, Asia, and Russia. The predominant representation was from the U.S. and the EU. The meeting focused on several topics, including:

- Model Validation
- Turbulence and Transport in the Core-Edge Transition Region
- Turbulence and Transport in 3D Systems
- Impurity Transport
- JEX/JAC 2011 Summaries and 2012 Proposals

Model Validation

Time-dependent transport simulations of current ramps (up and down) for ASDEX Upgrade discharges, together with analysis of gyrokinetic linear stability characteristics and how these evolve during the ramps were presented. The predictive transport simulations found that the GLF23 code provides insufficient diffusivity in the colder plasma periphery, and several theoretically-motivated simple 'patches' were invoked to improve the fit to the data. The gyrokinetic linear stability analysis indicates that ion temperature gradient (ITG) modes are dominant across most of the plasma during most of the rampup; trapped electron modes (TEM) dominate across the plasma early in the rampup, and in the central region when central electron cyclotron heating (ECH) is applied. New ASTRA & CRONOS simulations of a DIII-D discharge with an ITER-similar current-ramp were presented. Unlike simulations of JET, using a flat Z_{eff} profile with measured Te(r) to predict the evolution of the central safety factor is compatible with the experimental analysis by the EFIT code and avoids prematurely reaching q=1. Z_{eff} profiles will need to be reliably measured in order to enable validation of current evolution simulations. The TGLF transport model by itself was shown to have insufficient thermal diffusivity to predict the measured T_e in the colder periphery of the DIII-D, JET, and C-Mod plasmas that were used as a basis for the simulations. Adding the paleoclassical model improves agreement, but additional thermal diffusivity is still needed near the edge.

Core-Edge Transition

The focus of this subgroup is to attempt to understand the physics of the transition region between the core plasma and the plasma that forms the pedestal/edge. Are they two regions controlled by different processes, and how can we understand their connection? The EMEDGE3D code was applied to studying the formation of a transport barrier at the edge and the stability in the presence of resonant magnetic perturbations (RMPs). The code predicts unstable resistive ballooning modes (RBMs) in the edge in representative plasmas, with an increase in high frequency, but decrease in low frequency, turbulence in the presence of RMPs. The RBM was able to reproduce relaxations similar to edge localized modes (ELMs). The GENE code was used to assess the stability of RBMs in Tore-Supra L-mode plasmas. The RBM was found to be stable in these plasmas, except when collisionality was increased to high values. In this case, the mode was found only at the very edge, r/a~0.95. Theoretical work showed that electron driven geodesic acoustic modes (eGAMs) are induced by electron temperature gradient modes (ETGs) through energy cascades from short to long wavelengths. The eGAMs in turn set the radial scale of the ETG streamers, and can give an anomalous particle pinch in the edge pedestal of H-modes. A gyrokinetic analysis of the evolution of the H-mode pedestal during an ELM cycle on MAST was presented. The simulations showed that the microtearing mode dominated in the edge of the core plasma, but kinetic ballooning modes (KBMs) dominate through the width of the pedestal. These modes appear to be unstable just before the ELM crash, but it is still believed that peeling-ballooning is still the ELM trigger.

Transport in 3D Systems

This session was devoted to transport and turbulence issues in 3D systems, which included both stellarators and tokamaks. It was shown that open stochastic volumes from the 3D fields shared similarities on both types of devices in terms of the radial and poloidal transport. While applied RMPs caused particle pump-out in DIII-D, they could cause either pump-out or an improvement in particle confinement in TEXTOR, indicating the possible importance of the interaction between the RMPs and certain resonant flux surfaces. In LHD, the electron temperature is affected differently with different phases of the Local Island Divertor, indicating that the 1/1 island has a strong influence on confinement. Turbulence levels decreased in the case of a “healed” island. The dynamics between profile density gradients and transport during intermittent bursts of turbulence was studied, and it was found that both turbulence and transport was bursty. By looking at the probability distribution functions (PDFs) of the turbulence and density profile, the strongest turbulence events occurred when the density gradient was either above or below its most probable value. This may suggest that a non-local mechanism is operative. A comparison between gyrokinetic calculation results and turbulence characteristics as measured by phase contrast imaging (PCI) in LHD was shown. An axis shift in LHD led to different density profiles, peaked and hollow, with the peaked cases showing electron-direction turbulence dominating and hollow profiles being associated with turbulence in the ion direction. GS2 calculations showed that ion direction turbulence for both profile regimes; however, there was a smaller real frequency and shift toward the electron direction for the peaked density profile case, indicating a larger TEM contribution. This qualitatively agrees with the measurements. Nonlinear simulations of ion heat transport using the GKV-X code were done in the core-edge transition region (rho=0.4-0.8), and good agreement was found between experiments and simulations. 3D turbulence and transport effects in DIII-D with applied RMP were presented. With application of RMP, particle transport increased along with the low-k turbulence. The change in turbulence occurred on a fast time scale (~msecs) to the change in I-coil current, and it appears that the change in turbulence may be leading the change in gradients. The 3D subgroup will be refining specific questions to be posed in order to identify a specific Joint Experiment that can be carried out between tokamaks and stellarators. It is conceivable that this has overlap with the Pedestal group.

Impurity Transport

In the session dedicated to impurity transport, measurements of boron density profiles in ASDEX Upgrade, and related modeling with the gyrokinetic code GS2 and the neoclassical transport code NCLASS were presented by C. Angioni. The B density profiles in NBI heated H-modes exhibit an increase of peaking with increasing additional electron cyclotron heating (ECH) power, which correlates with the increase of Te/Ti, the reduction of toroidal rotation, and the reduction of the ion temperature gradient. First observations of He density profiles at JET in L-mode and H-mode standard and hybrid scenarios are found to be more peaked than the corresponding C density profiles, and as peaked as or more peaked than the electron density. First measurements of B and He density profiles in C-Mod were presented. Boron measurements cover all confinement modes and show clearly non-neoclassical behavior around mid-radius, where hollow density profiles are observed. Global nonlinear GYRO simulations of impurity transport in C-Mod demonstrate that predicted low Z impurities exhibit less peaking than hydrogen, but high Z impurities show significantly larger peaking in the more central region of the simulation domain.

JEX/JAC 2011 Summaries and 2012 Proposals

The final session involved the 2011 Summaries and 2012 Proposals for the Joint Experiments and Activities. About 4 JEXs will be closed out, with papers given at either the H-mode workshop and upcoming EPS or IAEA meetings. Three new activities were proposed. They include

1. L-H and H-L simulations. The aim of this is to build up a physics basis for modeling the transport evolution after the transitions (mostly H-L at first) to feed into the integrated modeling of plasma control. (D. McDonald)
2. Study of transition from LOC to SOC regime. There is new evidence that this may be associated with rotation reversals, and present-day turbulence diagnostics may bring new information on this topic. This activity would also involve gyrokinetic simulations, which would couple to the theory community. (J. Rice)
3. Non-local transport. Some of the aspects of this work are related to the LOC/SOC transition work. Scoping out studies (*i.e.*, data mining) will be carried out this coming year. A key motivation for revisiting this topic is the availability of turbulence data over a range of devices and enhanced computational capabilities. (H. Sun)

This is the final meeting that S. Kaye will be chairing. The new Chair of this group is Darren McDonald from JET.

Summary Report of the 21st Meeting of the ITPA Pedestal and Edge Physics Topical Group

Rajesh Maingi *(Oak Ridge National Laboratory),* ***Phil Snyder*** *(General Atomics), and* ***Howard Wilson*** *(U. York)*

The 21st meeting of the ITPA Pedestal and Edge Physics Topical Group was hosted by the York Plasma Institute at the University of York during 5-7 October 2011. The meeting reviewed new physics results on pedestal structure, edge localized mode (ELM) physics and modeling, pellet pacemaking, pedestal transport, ELM control, low and high confinement mode (LH) physics, and resonant magnetic perturbation (RMP) ELM control. The status and plans of the joint experiments were reviewed, and possibilities for new experiments discussed. The progress of the working groups that focus on the ITER urgent issues was reviewed; these are RMP ELM control, pellet pacemaking, toroidal field (TF) ripple, pedestal structure and LH physics. The contributions of the pedestal group to the cross-ITPA working group on density transport were discussed. X Gao offered to host the next (22^{nd}) meeting of the series at Hefei, China, from 2-4 April 2012.

Pedestal structure

J. Hughes reported on recent experimental results on Alcator C-Mod H-mode and I-mode pedestals, and described efforts to model the pedestal in H-mode. Initial ELITE calculations show that C-Mod ELMy H-modes operate near stability limits for ideal peeling-ballooning modes (PBM), as expected from the current understanding of Type I ELMs. Enhanced D-Alpha (EDA) H-mode discharges, on the other hand, are found ideal MHD stable by both ELITE and BOUT++, although BOUT++ does identify finite growth rates for edge modes with toroidal mode number *n* less than 30, when realistic values of resistivity and diamagnetism are included. Experimental C-Mod studies have provided additional supporting evidence for pedestal width scaling in ELMy H-mode as the square root of poloidal beta at the pedestal top; this is the dependence that would be expected from theory if kinetic ballooning modes (KBMs) were responsible for limiting the pedestal width. Studies of the pedestal and associated fluctuating fields in I-mode have continued. Temperature pedestal formation in I-mode is associated with a suppression of turbulence in the range of 60—150kHz, with an increase in fluctuations in the 200—300kHz range (the appearance of the weakly coherent mode, or WCM). The reduction of mid-range turbulence is well correlated with a substantial decrease in effective thermal diffusivity and the formation of the temperature pedestal with no density pedestal. In addition to clear fluctuations in the edge density and magnetic field, a ~1% $\delta T_e/T_e$ fluctuation has now been confirmed using the electron cyclotron emission (ECE) diagnostic in optically thick edge plasma.

R. Vann described the design, installation and first results from a novel microwave imaging system on MAST based on a phased-array technique. The ultimate objective is to make time-resolved measurements of the pitch angle and thence current density in the pedestal with very fast time resolution. In particular, this diagnostic is expected to provide a pedestal current density throughout the pedestal evolution between ELMs, right up to the ELM and immediately after it. First 2-D images of electron Bernstein wave- X-O mode conversion were presented, which characterize the magnetic field pitch angle at the position of the mode conversion. Work on back-transforming these more recent 2-D observations is under way to calculate the magnetic field structure and, from this, the current density across the pedestal.

P. Snyder presented the EPED model, which predicts the H-mode pedestal height and width based upon two constraints: 1) onset of non-local PBMs at low to intermediate mode number, 2) onset of nearly local KBMs at high mode number. Calculation of these two constraints using sets of model equilibria allows prediction of both pedestal height and width in terms of a simple set of scalar input parameters. The model, which has no adjustable parameters, has been successfully tested against observations for 273 cases from 5 tokamaks, finding a ratio of predicted to observed pedestal pressure of 1.00 ± 0.22, with a correlation of 0.91. A new higher resolution Thomson scattering system was implemented on DIII-D for 2011, and good agreement with EPED has been found in initial comparisons of pedestal width and height. Promising predictions and initial optimizations for ITER were presented.

D. Dickinson presented new calculations using the GS2 code on the linear gyrokinetic stability of the MAST pedestal between two ELM cycles. Both KBMs and microtearing modes are found to be unstable in the region $0.94<\psi_N<0.99$. In particular the KBMs are found in the steep gradient region whilst microtearing modes exist at the top of the pedestal where the gradient is shallower. A comparison with n=infinity ideal MHD ballooning modes indicates that the region unstable to KBMs is well described by the region unstable to n=infinity ideal MHD modes in this case. It is seen that steepening density gradients can suppress the microtearing modes before driving KBMs. Immediately prior to the ELM crash the pedestal top is near to a position in (β, β') where both KBMs and microtearing modes are simultaneously unstable over a large range of wavenumbers.

X. Xu covered two topics: BOUT++ 5-field simulations of pedestal stability and preliminary gyrokinetic stability calculations using the codes GEM and GYRO. The BOUT++ results illustrate the stabilization caused by diamagnetic effects, and this appears to be somewhat stronger in lower density discharges. Gyrokinetic stability analyses of the pedestal indicate good agreement between GEM and GYRO in some regimes, but differences in others. At the 95% surface of a DIII-D discharge, there appears to be a strong ion temperature gradient (ITG) mode.

R. Maingi described the improvement in H-mode and pedestal performance in NSTX with lithium wall coatings. Such coatings have been shown to reduce recycling, improve energy confinement, and suppress ELMs. New analyses show that these effects depend *continuously* on the amount of pre-discharge lithium evaporation. Specifically a nearly monotonic reduction in recycling is observed, together with a decrease in edge electron transport, and a modification of the edge profiles and stability with increasing lithium. These correlations challenge basic expectations, given that even the smallest coatings (range: 30-300 nm) exceeded that needed for a nominal thickness of order the divertor ion implantation range (< 10 nm).

P. Snyder summarized progress by the pedestal structure working group, showing highlights from the 2011 US joint research target on pedestal structure. The work on the pedestal width scaling confirms that any dependence of the width on ρ_* is weak. Furthermore, there is growing confidence in the EPED series of pedestal width models for ITER predictions. There is significant activity on gyrokinetic stability calculations of the pedestal (with several presentations at this meeting) that could feed into this, and a role of the ITPA pedestal group could be to help provide coordination of this effort. EPED only provides a pressure pedestal width: to break this down into density and temperature pedestal widths requires an understanding of the density transport, including whether or not a pinch operates, and sources. Concerning the impact of different heating mixes on pedestal physics, this depends on the phenomena under study. For example, the EPED model appears to work equally well across a range of heating, while some types of heating influence density transport in different ways that are not yet understood (e.g. lower hybrid on C-Mod causes density pump-out). The quiescent high confinement (QH) mode and its relevance to ITER is a topic explored by this group. The EPED1 model predicts that ITER pedestals will have access to QH mode (in principle) across a range of densities. The required momentum injection to generate QH mode is still an open question, but there are promising results from DIII-D that produce QH mode with zero NBI torque (instead making use of the neoclassical toroidal viscosity (NTV) torque provided by non-resonant magnetic perturbations).

ELM Physics and Modeling

G. Huysmans presented his latest results from the nonlinear MHD code JOREK, focusing on an understanding of the broadening of the ELM heat load deposition width (compared to the inter-ELM deposition width). He observes a similar broadening of the wetted area to that seen in experiment, which appears to be a consequence of the filaments in the simulation. Homoclinic tangles are clear in the simulations, and these define a minimum broadening of the strike-point.

B. Dudson described the latest ELM simulation results from BOUT++. His results showed that reconnection seems to play a role in the ELM physics and, in particular, in the termination of the ELM crash. Perhaps related to this, while the modes have a ballooning parity during the linear phase, they develop a growing tearing parity structure during the nonlinear phase. Results from an extension of the ideal MHD model to include a Hall term and electron inertia were presented, showing around a factor of two reduction in linear growth rate compared to ideal MHD (diamagnetic effects were not included).

G. Yun showed data on ELM dynamics from the new ECE imaging diagnostic on KSTAR. He showed the formation of a sinusoidal oscillation during an initial (linear) precursor phase, which then saturates in amplitude before the ELM eruption occurs with a series of bursting events. The ECE imaging (ECEi) system shows the bursts correspond to filaments erupting into the scrape-off layer. Application of an n=1 RMP on KSTAR initially triggers ELMs, and then leads to suppression. Two possible explanations that are being explored are (1) whether the RMP has a direct impact on the ELM dynamics, or (2) whether the impact of the RMP on the plasma shape is the dominant effect (e.g., through particle recycling).

E. Wolfrum described experiments on AUG to identify the characteristics of Type 2 ELMs and to explore whether there is any relation between them and the grassy ELMs that were observed on JT-60U. The type 2 ELM regime is associated with high triangularity and occurs above a critical collisionality, which, on AUG, is around 1. A comparison of the profiles between (pre-ELM) Type 1 and Type 2 discharges showed little difference in the density gradient of the pedestal, but ~30% lower temperature gradient (in Type 2). ECE indicates that the reduced temperature gradient is related to fluctuations, which actually penetrate beyond the pedestal into the plasma.

N. Oyama reviewed the status and plans for the TF ripple working group. The toroidal torque induced by fast ion losses due to the ripple had been evaluated using the ASCOT code, and validated by dedicated JET experiments. Calculations for the ripple induced thermal ion losses for ITER (scenario 2) had also been evaluated using the F3D-OFMC code. It was found that the additional losses in the case of 3 test blanket module (TBM) ports are below 1% of the number of test particles. These losses increase with the number of TBM ports and with the square of the amplitude of the local TF ripple.

RMP ELM control

Wolfgang Suttrop gave an update on ELM mitigation with the new in-vessel saddle coils on AUG. Experiments this year have been with two rows (top and bottom, off mid-plane) of four coils, with these presently being upgraded to two rows of eight coils ready for operation early in 2012. These experiments at relatively high collisionality show that application of the RMP causes the Type I ELMs to be replaced by frequent, small ELMs, but no density pump-out nor substantial stored energy loss is observed. Intriguingly the access to this mitigated ELM regime does not appear to depend on a resonance condition. The threshold density required for ELM mitigation can be achieved either by pellet or gas fuelling. Pellets are not seen to trigger large ELMs in the magnetic perturbation-mitigated phase. Pellets allow peaked density profiles to be achieved, with line-averaged density well in excess of the Greenwald limit. An interesting feature is that these high density, pellet-fuelled, magnetic perturbation ELM-mitigated discharges have a confinement time that does not increase with density, as expected from scaling laws. Discharges heated by NBI were compared with those heated by RF; magnetic perturbations had a similar effect in mitigating ELMs in both cases. The magnetic perturbations had little effect on plasma rotation, although a pre-existing mode can be slowed down. A scan of the safety factor q at the 95% flux radius (q95) showed that the density threshold cannot be interpreted as a minimum collisionality for mitigation. Also, ELM mitigation could not be achieved at low density and low q95.

M. Fenstermacher described recent results from DIII-D ELM control experiments, including RMP and QH-mode. These include: 1) ELM suppression at low collisionality for many energy confinement times using n=2 fields with optimized toroidal phasing, 2) synchronous response of signals on many diagnostics, to application of toroidally rotating n=2 RMPs, 3) direct comparison of the ELM response to n=3 RMPs in well matched plasmas having q95 differing by 0.1 in which ELM suppression was achieved throughout the discharge for q95=3.45 and ELM mitigation was achieved for q95=3.55, and 4) comparison of the ELM response in well matched plasmas with variation in up/down equilibrium balance (δ_r^{sep}) in which ELM suppression was obtained for δ_r^{sep}=-4 cm and ELM mitigation was obtained for δ_r^{sep} =-2cm and in symmetric double null (DN) shape. Results from experiments with QH-mode operation showed 1) extension of the operating space to net positive torque up to 1.5 Nm (about 4x the positive torque projected for ITER) using n=3 non-resonant magnetic fields (NRMFs) from both the internal and external coils on DIII-D, and 2) QH-mode achieved with zero input torque using NRMFs from the external coils alone.

Y. Suzuki described work reconstructing 3D tokamak equilibria using the HINT2 code. This code evolves resistive MHD equations towards a steady state, to derive the equilibrium magnetic field structure in the plasma, without the assumption of nested flux surfaces. Analyzing a DIII-D equilibrium, he compared the full plasma equilibrium with a vacuum solution, showing similar solutions for both the shapes of the flux surfaces and the positions and phases of the magnetic islands. The level of stochastization is influenced by the plasma response.

S.-W. Yoon showed a variety of ELM suppression/mitigation studies on KSTAR, with a variety of techniques. Application of n=1 RMP coils provided complete suppression of ELMs, following an initial phase where the coils actually excited ELMs. A density pump-out is observed as the coils are first applied, but the density then begins to recover once the ELMs are suppressed. Likewise, initially there is a drop in the toroidal rotation up until the point when the ELMs are suppressed, after which the rotation is maintained. Another ELM control technique presented was electron cyclotron resonance heating (ECRH) into the pedestal region. The ELM frequency was found to approximately double (from around 20Hz to 40Hz), accompanied by a drop in density and rotation. The use of supersonic molecular beam injection (SMBI) influenced the ELMs, with evidence for smaller filaments, but also led to ~10% drop in stored energy. Finally a vertical jog of greater than ~1cm was found to trigger ELMs at the point of maximum velocity. Large vertical excursions triggered multiple ELMs.

A. Kirk gave an update on MAST RMP experiments. The positions of the divertor strike point lobes observed in the far SOL were found to be in good agreement with the predictions of vacuum modeling using the ERGOS code. ELM mitigation has been obtained in Lower Single Null Divertor type I ELMing plasma, when the RMPs are applied in an n=4 or n=6 configuration.

M. Becoulet described nonlinear MHD simulations of RMP error field penetration into a rotating plasma. She showed that penetration required the local electron flow speed across the magnetic field lines to be zero (i.e., the sum of ExB and electron diamagnetic flows). Simulations for JET showed that while the RMPs did penetrate the edge plasma region, the total electron velocity in the core is not zero, and the central islands are therefore screened. A similar result was found for ITER, where there was a substantial difference observed between the vacuum and plasma response calculations.

J. Callen presented his "magnetic flutter" model of radial plasma transport induced by RMPs, which is being developed to explore the possibility that these effects could reduce the electron pressure gradient at the top of the pedestal ($0.9 < \psi_N < 0.97$), and thereby keep the pedestal below the PBM stability boundary, even if flow screening prevents penetration of the RMP fields and hence magnetic stochastization. The RMP-induced radial diffusivities of electron heat and density are predicted to scale as the product of the parallel electron heat diffusivity and the relative magnitudes of the resonant and non-resonant RMP fields within the plasma. Preliminary results from this RMP flutter-induced transport model agree qualitatively with low collisionality DIII-D data regarding the magnitude and I-coil current scaling of the reduction in the electron temperature and density gradients at the pedestal top, and the factor of 3 larger effect on the electron temperature versus density gradient.

LH Transition Physics

D. Battaglia presented work on the role of ion orbit loss in the LH transition on NSTX. He pointed out that ions are lost near the X-point because the grad-B drift is enhanced there (the poloidal field goes to zero). This drives a negative radial electric field to retain the ions (X-transport theory). He looked at the critical energy required for ions to be lost, and found that it increases as the major radius of the X-point is decreased. This, in turn, requires a higher ion temperature. If one assumes the non-ambipolar ion loss drives the radial electric field, and that this electric field is what drives the L-H transition, then this result suggests a higher ion temperature (and therefore more heating) would be required to access the H-mode. Experiments on NSTX do indeed observe a higher power threshold with the X-point at smaller radius.

Pellet pacemaking

S. Futatani gave a presentation on modeling ELM triggering by pellets in DIII-D using the JOREK code. A pellet ablation model had been incorporated into JOREK, with first simulations aimed at validation for Tore Supra parameters. A toroidally symmetric ablation cloud has been assumed for now.

P. Lang gave an overview of the progress in addressing pellet pace-making issues for ITER on AUG and JET. Both JET and AUG indicate a minimum (yet to be quantified) pellet size requirement for triggering ELMs. Experiments on AUG showed that the fuelling efficiency of pellets was improved when Type I ELMs were mitigated with the magnetic perturbations, and indeed the fuelling pellets do not trigger ELMs in this regime. It was also shown that pellets could be used to provide the minimum density required for ELM mitigation with 3D fields. The ability to successfully trigger ELMs with pacing pellets immediately after the LH transition (i.e. before natural ELMs started) was demonstrated on AUG. On JET, the High Frequency Pellet Injector has been substantially improved and is being commissioned.

M. Fenstermacher (on behalf of **L. Baylor**) described the new LFS pellet injection line that had been installed on DIII-D and tested successfully. This injection line mimics the ITER plan for pellet ELM pacing with injection in the vicinity of the X-point. New data from this trajectory confirms ELM triggering before the pellet reaches the top of the pedestal. A new 1.3mm slow pellet injector was installed on one of the three injector lines and tested at 20 Hz. Initial piggyback tests show 1.3mm pellets trigger ELMs when injected from the low field side (LFS) midplane. Pellet fragments also appear to trigger ELMs when only 1ms apart.

Transport

J.-W. Ahn described 3D field effects in the divertor and pedestal of NSTX. A camera is able to view the full toroidal angle of the divertor, and reveals some toroidal asymmetries in the divertor heat flux even in quiet ELM-free discharges. ELMs can be triggered with n=1 and n=3 magnetic perturbations on NSTX, and these are found to be phase-locked with the perturbations. Vacuum calculations of the strike-point splitting are in good agreement with the observed splitting. A study of detachment showed that the application of 3D fields can partially re-attach the plasma in cases with weak gas fuelling. In stronger puffing scenarios, the pedestal temperature is prevented from increasing as the 3D fields are applied, and the plasma remains detached.

A. Diallo gave a presentation on turbulence and thermal transport in the pedestal region between ELMs on NSTX. Reflectometer measurements of the density fluctuations showed that the radial correlation length was found to increase during the last 50% of the ELM cycle, which may be a consequence of the observed widening of the pedestal region between ELMs. Although a definite identification cannot be made at this stage, the observed correlation lengths (several mm) are consistent with either ITG or KBM modes.

T. Rognlien presented modeling of edge profile evolution aimed to develop an understanding of particle transport. Time-dependent edge transport simulations with UEDGE were used to investigate the density buildup in the pedestal region. It is found that the very fast transport of the neutrals into the barrier with a modulated gas source does not allow a discernible difference between the time response of a solely diffusive transport, or one with a large local pinch.

A. Loarte continued the theme of transient density evolution in H-mode plasmas. This is important because if the density increases too fast in ITER, the ion temperature would be limited, constraining the fusion power; also high density would raise the LH transition power threshold. The pedestal plays a key role here: all density has to cross through this region from the edge to fuel the core. Understanding density transport in the pedestal is further complicated because of the need to understand the sources as well as the transport processes. Here, the LH transition was modeled either by a reduction in the particle diffusivity, or through a combination of a drop in diffusivity and an inwards pinch. The two approaches yield different shapes for the density profile in the pedestal that can be compared with experiment. Such a comparison with JET supports the existence of a density pinch.

Finally, **A. Pankin** described modeling of the electron thermal transport arising from electron temperature gradient (ETG) modes near the pedestal of DIII-D with the FACETS framework. He compared four models for ETG transport: Horton-Jenko, GLF23, TGLF and Gyro. Horton-Jenko and GLF23 both predict that ETG modes are unstable over the outer 50% of the plasma, while TGLF and Gyro predict a greater region is unstable, beyond ~30% of the normalized radius. The models give very different thermal diffusivities. For example, the GLF23 and Horton-Jenko models predict a maximum in the diffusivity near the pedestal top, while the maximum diffusivity predicted by TGLF is shifted towards the core.

Announcements

Submit BPO-related announcements for next month's eNews to [Dylan Brennan.]

Upcoming Burning Plasma Events

2011 Events

Dec 12-15, 2011
ITPA CC & CTP-ITPA Joint Experiments Meeting
Cadarache, FRANCE

2012 Events

Jan 16-19, 2012
ITPA Divertor and SOL (PSI Selection Committee) Topical Group Meeting
Jüelich, GERMANY

Mar 5-9, 2012 NEW
ITPA Energetic Particles Topical Group Meeting
NIFS, JAPAN

Mar 5-9, 2012 NEW
ITPA MHD Topical Group Meeting
NIFS, JAPAN

Apr 2-4, 2012
ITPA Pedestal and Edge Physics Topical Group Meeting
Hefei, CHINA

Apr 2-5, 2012 NEW
ITPA Transport and Confinement Topical Group Meeting
Hefei, CHINA

Apr 16-19, 2012 NEW
ITPA Integrated Operation Scenarios Topical Group Meeting
CIEMAT, Madrid, SPAIN

May 14-17, 2012 NEW
ITPA Diagnostics Topical Group Meeting
Kutchatov Institute, RUSSIA

Jul 8-12, 2012 NEW
39th IEEE International Conference on Plasma Science (ICOPS2012)
Edinburg, UNITED KINGDOM

Oct 8-13, 2012
24^{th} IAEA Fusion Energy Conference
San Diego, CA

Directories of Other Plasma Events

IEEE Directory of Plasma Conferences
Fusion Ignition Research Experiment (FIRE) Physics Meetings
Fusion Power Associates Meetings Calendar

Please contact the administrator with additions and corrections.